

Magnetoresistance of junctions made of underdoped $\text{YBa}_2\text{Cu}_3\text{O}_y$ separated by a $\text{YBa}_2\text{Cu}_{2.6}\text{Ga}_{0.4}\text{O}_y$ barrier

L. Shkedy,* G. Koren, and E. Polturak

Physics Department, Technion - Israel Institute of Technology, Haifa, 32000, Israel

(Received 24 June 2004; revised manuscript received 11 November 2004; published 11 April 2005)

We report magnetoresistance measurements of ramp-type superconductor-normal-superconductor (*SNS*) junctions. The junctions consist of underdoped $\text{YBa}_2\text{Cu}_3\text{O}_y$ (YBCO) electrodes separated by a barrier of $\text{YBa}_2\text{Cu}_{2.6}\text{Ga}_{0.4}\text{O}_y$. We observe a large positive magnetoresistance, linear in the field. We suggest that this unusual magnetoresistance originates in the field dependence of the proximity effect. Our results indicate that in underdoped YBCO-N-YBCO *SNS* structures, the proximity effect does not exhibit the anomalously long range found in optimally doped YBCO structures. From our data we obtain the diffusion coefficient and relaxation time of quasiparticles in underdoped YBCO.

DOI: 10.1103/PhysRevB.71.134502

PACS number(s): 74.45.+c, 74.25.Ha

I. INTRODUCTION

In the usual description of the proximity effect, when a superconductor (*S*) is brought into contact with a normal conductor (*N*), the order parameter (*OP*) in the superconductor is depressed near the interface and superconductivity is induced in *N*. The pair amplitude induced in *N* decays on a length scale K^{-1} from the interface, called the decay length.¹⁻³ In *SNS* junctions in which *S* is an optimally doped High Temperature Superconductor (HTSC) and *N* belongs to the same material family, but is doped to be nonsuperconducting, the decay of the pair amplitude in *N* typically takes place over a rather long distance of tens of nm.⁴⁻⁶ In contrast, if both *S* and *N* are underdoped cuprates, the pair amplitude in *N* seems to decay over a much shorter distance, on the order of a few nanometers. We have observed this effect in underdoped $\text{YBa}_2\text{Cu}_3\text{O}_y$ (YBCO) based junctions⁷⁻⁹ having a barrier made of $\text{YBa}_2\text{Cu}_{2.55}\text{Fe}_{0.5}\text{O}_y$ or a $\text{YBa}_2\text{Cu}_{2.6}\text{Ga}_{0.4}\text{O}_y$. In *SNS* junctions having a barrier much thicker than the decay length, Cooper pairs cannot tunnel through and the junctions exhibit a finite resistance at all temperatures. Roughly speaking, superconductivity in *N* is induced near the two *SN* interfaces, while a section of length ℓ in the middle of the barrier remains normal. This is the type of junction studied in the present work.

We are not aware of previous investigations of the proximity effect in HTSC under a magnetic field. When a magnetic field is applied, superconductivity is reduced and penetrates less into the normal conductor. As a result, the proximity effect is field dependent.² If the superconductivity in the barrier is weakened, the length of the normal section in the junction should increase, and with it the junction's finite resistance. As a result, a positive magnetoresistance [MR, defined as $\text{MR} \equiv R(H) - R(0)$] should be observed. We indeed observed such MR, linear in the field. An attempt to explain this unusual field dependence is the subject of this paper.

Besides the field dependence of the proximity effect, there are several additional mechanisms that could contribute to the MR. These include flux flow in the superconducting electrodes,^{3,10} normal MR of the barrier material (which is caused by bending of electron trajectories),¹¹ field dependent

hopping in the barrier,^{12,13} and resonant tunneling between the electrodes across the barrier.¹⁴ In the following we show that the contribution of all these processes to the observed MR is insignificant and we attribute it primarily to a field-dependent proximity effect in the barrier.

II. EXPERIMENTAL

The junctions used in the present study are thin film-based ramp junctions of the type that was previously used in our work.⁶ The junctions consist of two underdoped superconducting YBCO electrodes separated by a thin layer of $\text{YBa}_2\text{Cu}_3\text{Ga}_{0.4}\text{O}_y$ (Ga-doped YBCO) barrier. Ga has no magnetic properties. The transport current flows in the *a-b* plane through the Ga-doped YBCO layer. The multistep process of junction preparation by laser ablation was described previously.⁷ Briefly, we first deposit a 100 nm thick *c*-axis-oriented epitaxial YBCO layer onto a (100) SrTiO_3 (STO) substrate. This base electrode is then capped by a thick insulating layer of STO. Patterning is done by Ar ion milling to create shallow angle ramps along a main crystallographic direction in the *a-b* plane. In a second deposition step, the barrier layer, the YBCO cover electrode, and the Au electrical contacts are deposited, and then patterned to form the final junctions layout. This produces several junctions with 5 μm width on the wafer. Four terminal-resistance measurements of the junctions were carried out as a function of temperature and magnetic field of ≤ 8 Tesla. The field was perpendicular to the transport current, which in our geometry flows in the *a-b* plane of the films.

III. RESULTS AND DISCUSSION

Resistance versus temperature (*RT*) measurements of six junctions on the wafer are shown in Fig. 1. In the normal region, the difference in the resistance of the junctions is due to the different lengths of the YBCO leads. One observes two distinct superconducting transitions with T_c onset of 35 K and 53 K, which are attributed to each one of the electrodes. In the oxygen annealing process of underdoped YBCO, the oxygen concentration is kept low and the duration of the

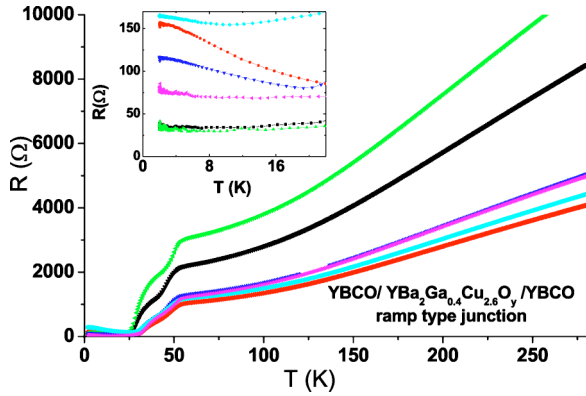


FIG. 1. (Color online) Resistance vs temperature of six junctions with 21 nm thick Ga-doped YBCO barrier. In the normal state, the different resistances of the junctions are due to different lengths of the YBCO leads. The inset shows the low temperature resistance of the junctions where both electrodes are superconducting.

annealing is relatively short. Consequently, the base electrode, which is covered by a thick layer of STO, absorbs less oxygen and its transition temperature is lower. Below about 30 K, both electrodes are superconducting and the inset of Fig. 1 shows the low temperature resistance of the junctions, which is due to the barrier. Qualitatively similar behavior was observed in edge junctions made of underdoped YBCO separated by a $\text{YBa}_2\text{Cu}_{2.55}\text{Fe}_{0.5}\text{O}_y$ barrier.^{7,8} The scatter of the values between different junctions is typical of our junction preparation process and is probably due to nonuniformities in the local Ga concentration and to variations in the transparency of the interfaces, most probably resulting from damage created by the ion milling of the ramp. The transparency of our junctions can be estimated from measurements of the critical current described below, which indicate that the transparency is low. The temperature dependence of the junction's resistance is typically weaker than that of the parent material in the form of a film, shown in Fig. 2. At low temperatures, the absolute resistivity of the junctions is also much smaller than that of a $\text{YBa}_2\text{Cu}_{2.6}\text{Ga}_{0.4}\text{O}_y$ film. One possible interpretation is that the thickness of the barrier (21 nm

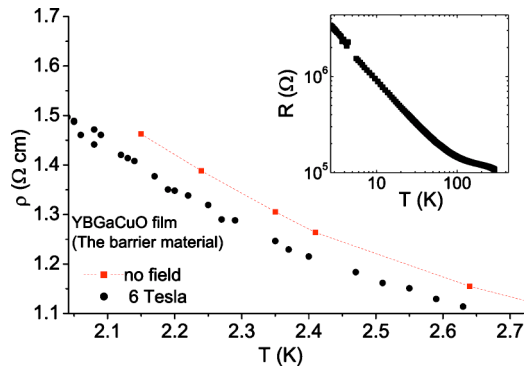


FIG. 2. (Color online) Resistivity vs temperature of 100 nm thick film of the Ga-doped YBCO material. Square symbols are measured at zero field and the circles are measured with 6 Tesla field applied perpendicular to the film. Note that the MR of the film is negative, in contrast to the positive MR of our junctions.

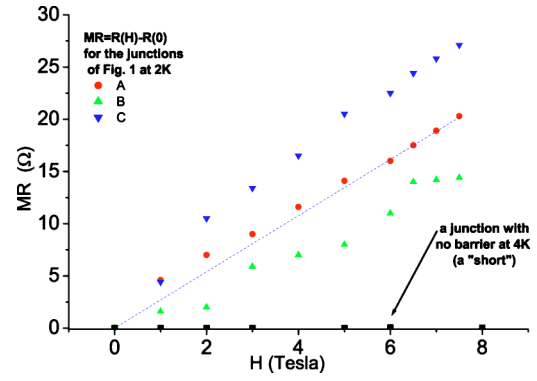


FIG. 3. (Color online) Magneto-resistance vs field of three of the junctions of Fig. 1 at 2 K, and of a “short” junction at 4 K. The “short” resistance is about 0.4Ω at 8 Tesla, which is almost two orders of magnitude smaller than the corresponding MR of the other junctions with a barrier. The dashed line is a guide to the eye.

in this work) is in the range where the material is mesoscopic. Under these conditions, the temperature dependence of the resistance is expected to be much weaker than that of a macroscopic film.¹⁵ The differences of the absolute resistivities between different junctions may perhaps result from different interface transparencies, which also affect the conductance of the device in the mesoscopic regime.¹⁵

Our main experimental result is shown in Fig. 3, where the measured magneto-resistance MR at low T is plotted as a function of magnetic field normal to the wafer. All junctions showed similar behavior. Detailed measurements were done on three of the six junctions on the wafer. One can see that all three junctions show a large positive MR, which is linear in the applied field. The MR typically reaches a value of $\sim 20 \Omega$ at 8 Tesla, which is larger than the resistance at $H = 0$ by tens of a percent.

We consider possible sources for the MR in our junctions. MR originating in the two YBCO electrodes below the superconducting transition temperature can result, for instance, from flux motion. This contribution would be linear in the field. In order to estimate the size of this contribution, we performed low-temperature MR measurements on bare YBCO microbridges. At temperatures close to T_c , flux flow was indeed observed (see the Appendix). However, at low temperatures where the junctions of Fig. 3 were measured, no measurable MR was observed in the thin-film YBCO microbridges. Therefore, flux flow in the YBCO electrodes does not contribute to the MR. We also measured the MR of junctions prepared in the same way, but without the barrier layer. These junctions are referred to as “shorts.” As shown in Fig. 3, under similar bias currents and fields, the “shorts” did exhibit a small MR of about 0.4Ω at 8 Tesla. The “shorts” show a finite MR since the interface between the two YBCO electrodes is always imperfect. The MR of the “shorts” is smaller than the MR in the junctions by almost two orders of magnitude. The interface resistance cannot be directly measured. What can be measured is the critical current density. Typically, the critical current density at low temperature of a 60 K YBCO “short” is one order of magnitude smaller than that of a film. This implies that the transparency of our junctions is low. To summarize this section, the above

series of control experiments show that MR in the electrodes is *not* the source of the large MR observed in our junctions.

A second potential source for the observed MR in Fig. 3 could be the barrier material itself. We therefore measured the MR of the Ga-doped YBCO. Specifically, we measured the resistance versus temperature of microbridges patterned in a thin film of this material annealed under the same conditions as the junctions in Fig. 3. Figure 2 shows the resistivity of these bridges with and without magnetic field. The barrier material exhibits a clear *negative* MR of $\sim 5\%$ at 2 K. The sign of this MR is opposite to that of the junctions, which show a large *positive* MR. At low temperatures, where the MR of the Ga-doped films is largest, the MR contributed by the barrier in the junctions would be at most -8Ω (5% of 160Ω , as seen in the inset of Fig. 1). However, since the sign of the MR of the barrier material itself is negative, the net (positive) MR of the junctions should be even larger than shown in Fig. 3. Consequently, the properties of the barrier material on its own cannot explain the observed MR of the junctions.

The above-mentioned control experiments clearly show that the MR of our junctions does not originate from the superconducting electrodes nor from the normal properties of the barrier material. The net MR that we see has a magnitude characteristic of the transition of part of the barrier from a superconducting to a normal state. We therefore examine whether the MR could originate from the depression of superconductivity near the *SN* interface of the junction.

Before going into a more detailed analysis, we note that our barrier is a mesoscopic section of a Mott insulator (MI), with the conductance of the material in bulk form showing variable range hopping.¹⁶ Its low temperature resistivity, $0.8 \Omega \text{ cm}$, is about three orders of magnitude larger than the maximum resistivity of metals (Mott-Ioffe-Regel limit²⁰). Strictly speaking, our junctions are *S/MI/S* junctions. So, the application of the usual theoretical description of the proximity effect to our junctions is not *a priori* justified, since both the de Gennes and Usadel equations are valid only for dirty metals. However, it is an experimental fact that when an MI with resistivity $\rho \leq 1 \Omega \text{ cm}$ is in good electrical contact with a superconductor it behaves similarly to a metal.^{16,21–23} The question of which particular model to use is therefore a matter of choice. In the limit of small induced pair amplitude in *N*, which applies to our low-transparency junctions, the de Gennes and Usadel approaches give the same result. Since the de Gennes approach was traditionally employed in all previous and current work on HTSC proximity structures,^{4,5,24} we prefer to follow this route. In any case, the analysis presented below is, nevertheless, useful in terms of assigning values to physical quantities, such as the decay length, which can then be intercompared between different experiments.

We first discuss the MR on the *S* side of the *SN* interface. In this region, the order parameter is reduced, superconductivity is depressed, pinning is weakened, and flux flow could occur despite the low temperature. We now estimate the upper limit on the contribution of this effect to the MR. The low temperature normal state resistivity of YBCO, extrapolated from the linear part of the *RT* plot above the transition, is about $10^{-4} \Omega \text{ cm}$. An upper limit on the volume near the

interface in which superconductivity is weakened is $10\xi \times A \sim 200 \text{ \AA} \times 0.5 \mu\text{m}^2$, where A is the junction cross section.¹⁹ The normal state resistance of this region is very low, less than 0.1Ω . Since the flux flow resistance is a fraction of the normal state resistance, it follows that the MR in the *S* side close to the interface is negligible.

Turning now to the *N* side of the interface, the resistivity of the barrier material is quite high, $0.8 \Omega \text{ cm}$ at 2 K. A rough estimate done assuming Ohm's law in the barrier indicates that a 1 nm thick slice of the barrier has a resistance of $R \sim 16 \Omega$. This value is similar to the total MR seen in Fig. 3. In the following, we propose that the observed MR is caused by changes in the effective penetration of superconductivity into the barrier. In other words, when a magnetic field is applied, the magnitude of the pair amplitude induced in the barrier is decreased and ℓ , the effective length of the barrier, which remains normal, increases thus increasing the resistance of the junction.

The magnetic fields used in the present study are small compared to H_{c2} of the 60 K YBCO phase which is 50 T.¹⁸ Thus changes in the minigap Δ due to the applied field are also small but not negligible. The value of Δ on the *S* side near the interface is proportional to T_c , which itself depends on the magnetic field due to pair breaking according to^{3,17}

$$\ln\left(\frac{T_c}{T_{c0}}\right) = \Psi\left(\frac{1}{2}\right) - \Psi\left(\frac{1}{2} + \frac{\alpha}{2\pi k_B T_c}\right), \quad (1)$$

where T_c is the critical temperature under applied field and T_{c0} is the critical temperature at zero field. Ψ is the di-Gamma function defined as $\Psi(x) = \Gamma'(x)/\Gamma(x)$ and α is the pair-breaking parameter. For a thin film under a perpendicular applied field $\alpha = D_S eH/c$, where D_S is the diffusion coefficient in the superconductor. Because the highest magnetic field we used is small compared to H_{c2} , pair breaking is small and $(\alpha/2\pi k_B T_c)$ is a small parameter. In this limit, Eq. (1) reduces to^{3,17}

$$k_B(T_{c0} - T_c) = \frac{\pi\alpha}{4}. \quad (2)$$

From our *RT* measurements under different fields we find the values of T_{c0} and T_c (65 K at 0 T and 55 K at 7 T, respectively). We can thus calculate the value of α , which is $\sim 1 \text{ meV}$ at 7 Tesla. Therefore, $\alpha/2\pi k_B T_c \approx 1/35$, and this justifies the use of Eq. (2). By assuming a linear scaling between Δ and T_c ($2\Delta = \beta k_B T_c$, with β being a constant of about 5), we estimate that under a field of 7 T the magnitude of Δ decreases by about 15%. The suppression of Δ can therefore be written as

$$\delta_S \equiv \Delta_S(0) - \Delta_S(H) = \frac{\pi\alpha\beta}{8} = \frac{\pi\beta D_S eH}{8c}, \quad (3)$$

where δ_S is small compared to $\Delta_S(0)$. The spatial dependence of the Δ in a *SNS* junction is shown schematically in Fig. 4. The value of the Δ on both sides of the interface is related through the standard boundary condition^{2,3}

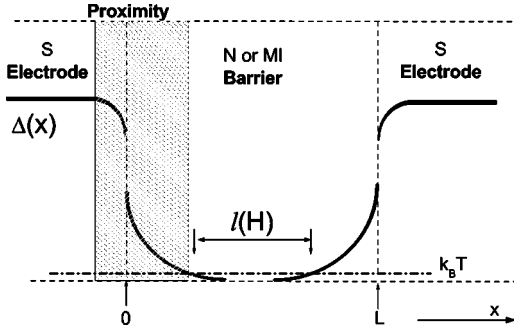


FIG. 4. Schematic diagram of the junction and the spatial profile of $\Delta(x)$. $\ell(H)$ is the length of the resistive region of the junction. The shaded area shows the region in which superconductivity is weakened on both sides of the interface due to the proximity effect.

$$\left(\frac{\Delta_S^i}{N_S V_S} \right)_{x=0} = \left(\frac{\Delta_N^i}{N_N V_N} \right)_{x=0}, \quad (4)$$

where Δ_S^i and Δ_N^i are the values of the minigap at the S and N sides of the SN interface. N_S and N_N are the normal state density of states (DOS) on the S and N sides of the interface, respectively. Finally, V_S and V_N are the electron-electron interaction on the S and N sides. Assuming the DOS and the electron-electron interaction are field independent we obtain

$$\frac{\Delta_S^i(H)}{\Delta_N^i(H)} = \epsilon = \frac{\delta_S^i}{\delta_N^i}, \quad (5)$$

where $\epsilon = N_S V_S / N_N V_N$ is a field-independent constant and we define $\delta_N^i \equiv \Delta_N^i(0) - \Delta_N^i(H)$. δ_N^i , which is the value at the interface, is also a small parameter as $\delta_N^i / \Delta_N^i(0) \ll 1$.

Turning to the N side now, under a magnetic field H applied in the c direction, the spatial dependence of Δ is given by the linearized Ginzburg-Landau (GL) equation²

$$-\frac{d^2 \Delta_N}{dx^2} + \left(\frac{2eH}{\hbar c} \right)^2 (x_0 - x)^2 \Delta_N + K^2 \Delta_N = 0, \quad (6)$$

where x_0 and K are constants. In our experiment, $x_0 - x$ is limited by 10 nm, which is half the thickness of our junction, the field H is less than 8 T, and K is on the order of a few nanometers. Using these parameters, we estimate that the upper limit of the second term in Eq. (8) is about two orders of magnitude smaller than the last term. In this limit, the solution of Eq. (8) for Δ in N exhibits an exponential decay with distance $\Delta_N(x) = \Delta_N^i \exp(-Kx)$. In the dirty limit,² K is given by

$$K^{-1} = \left(\frac{\hbar D_N}{2\pi k_B T} \right)^{1/2}. \quad (7)$$

In this limit, where the cyclotron radius in the magnetic field is much larger than the mean-free path, D_N is field independent and thus K does not depend on field. However, the value of Δ at the interface Δ_N^i is field dependent because it is pinned to the value of the Δ on the S side at the interface, Δ_S^i through Eq. (5). The pair amplitude induced in the barrier is effectively depressed to zero by thermal fluctuations at some distance from the interface, and from that distance onward

the material has a finite resistance. The natural way to determine this distance is through the condition that the extrapolated magnitude of Δ there is of the order of $k_B T$. This length, which we denote by X , depends on the field as

$$k_B T = \Delta_N^i(H) e^{-KX(H)}, \quad (8)$$

where $X(H)$ is the effective penetration depth of superconductivity into N when a magnetic field is applied. Dividing $X(H)$ by $X(H=0)$ we find

$$\frac{\Delta_N^i(0)}{\Delta_N^i(H)} = e^{K[X(0) - X(H)]} \quad (9)$$

and

$$X(H) - X(0) = \frac{1}{K} \ln \left(1 - \frac{\delta_N^i}{\Delta_N^i(0)} \right). \quad (10)$$

Since δ_N^i is a small parameter $X(H) - X(0) \sim -\delta_N^i / K \Delta_N^i(0)$. Referring to the schematic model shown in Fig. 4, the field-dependent resistance of the barrier is $R = \rho \ell(H) / A$, where $\ell(H) = L - 2X(H)$ is the length inside the barrier, which is normal. Using Eq. (5) and the relation $2\Delta_S = \beta k_B T_c$, the magnetoresistance comes out as

$$\text{MR} \equiv R(H) - R(0) = -2 \frac{\rho}{A} [X(H) - X(0)] = \frac{\pi \rho e D_S}{2cAK} \left(\frac{1}{k_B T_c} \right) H. \quad (11)$$

We therefore see that the MR is linear in H , in agreement with the observed behavior in Fig. 2.

A rough estimate of the decay length ($1/K$) in the underdoped barrier at low temperature can be attempted using the resistivity of the barrier, 0.8 Ω cm and the typical resistance of the junctions $\sim 100 \Omega$. Using these values, we estimate the length of the barrier which remains normal $\ell(H=0)$ as 6 nm. Taking the thickness of the barrier of 21 nm and assuming that the pair amplitude decays to zero over three times the decay length ($1/K$), we obtain a value for $1/K$ of about 2.5 nm. $1/K$ can also be calculated using Eq. (7), where $D_N = \frac{1}{3} \ell_N v_{FN}$. The mean-free path in the barrier can be estimated as the distance between nearest Ga atoms $\ell_N \sim 5 \text{ \AA}$ and the Fermi velocity in the barrier $v_{FN} = 1.2 \times 10^7$ cm/s was measured in a previous study.¹⁶ This yields $1/K \approx 3.5$ nm. It appears that both methods of estimating $1/K$ give values that are consistent. We note that the decay length estimated in underdoped SNS structure comes out much smaller than in optimally doped ones.^{4,5}

Using our data we estimate the diffusion coefficient D_S and the relaxation time τ_S of underdoped YBCO. Taking an average T_c of ~ 45 K and an average slope in Fig. 3 of $\text{MR}/H = 2.7 \Omega/\text{Tesla}$, Eq. (11) yields $D_S \sim 1 \text{ cm}^2/\text{s}$. This is consistent with an independent estimate that can be extracted from Eq. (2) and from the relation between α and the diffusion coefficient D_S which yields $\sim 1.7 \text{ cm}^2/\text{s}$. The relaxation time τ_S is extracted from the usual relation that connects it with the diffusion coefficient $D_S = \frac{1}{3} v_{FS}^2 \tau_S$, where v_{FS} is the Fermi velocity of quasiparticles in the superconductor $\sim 2 \times 10^7$ cm/s.²⁵ Under these assumptions τ_S for YBCO is ~ 25 fs. The value found for τ_S is of the same order of mag-

nitude as the recent results of Gedik *et al.*,²⁵ who obtained $\tau_S \sim 100$ fs, whereas our value of D_S is smaller than theirs, $D_S \sim 20$ cm²/s.

For completeness, we mention that Abrikosov has predicted another mechanism for linear MR versus H in superconductors.¹⁴ He assumed a field-dependent resonant tunneling, which yields MR linear in H at very high magnetic fields, when only a few Landau levels are filled. When the field is reduced and the number of filled Landau levels increases, the field dependence of the MR changes into a quadratic one. This model could, in principle, explain the observed linear behavior of our MR results. However, peaks in the density of states due to Landau levels are absent in the dynamic-resistance spectra of our junctions. Moreover, the fields used in our experiment are not high enough to reach the regime where a low number of Landau levels are filled. Hence, if this model was applicable to our junctions, we should have observed a quadratic dependence of the MR on field, which is not the case.

IV. CONCLUSIONS

We investigated the resistance of SNS structures based on underdoped YBCO with a nonmagnetic Ga-doped YBCO barrier as a function of magnetic field. We discovered a linear increase of the resistance with the field. An extensive series of control experiments indicates that this field dependence does not result from flux flow, which would be the obvious mechanism of MR in a superconductor. A simplified analysis indicates that the effect may well be explained by a field-dependent proximity effect in the barrier. This explanation produces a reasonable estimate of the diffusion coefficient and the relaxation time in YBCO. Furthermore, our estimates indicate that in underdoped YBCO SNS structures, the superconductivity induced inside the barrier through the proximity effect has a short (~ 2 – 3 nm) range, unlike the long-range proximity effect observed in optimally doped YBCO structures.

ACKNOWLEDGMENTS

We thank Pavel Aronov for the “short” junction data of Fig. 2. This research was supported in part by the Israel Science Foundation (Grant No. 1565/04), the Heinrich Hertz

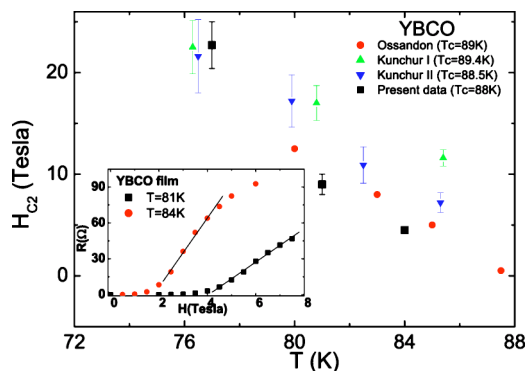


FIG. 5. (Color online) H_{c2} vs temperature of optimally doped YBCO film. H_{c2} was extracted from the slope of the linear part of the MR (inset) using the Bardeen-Stephen model. Our data (solid squares) can be compared to previous measurements by Kunchur *et al.* and Ossandon τ_S .^{27,28}

Minerva Center for HTSC, the Karl Stoll Chair in advanced materials, and by the Fund for the Promotion of Research at the Technion.

APPENDIX

For the sake of comparison to previous work, we also measured the MR of *optimally doped* YBCO films at temperatures close to T_c , as shown in the inset of Fig. 5. In this case, the resistance showed a region linear with an applied field. In the Bardeen-Stephen model,^{3,10,26} the resistance resulting from flux flow is given by $R_{\text{flux flow}} = [H/H_{c2}(T)] \times R_N(T)$, where H is the applied magnetic field and $R_N(T)$ is the normal state resistance at temperature T , extrapolated from the RT plot close to T_c . Using this model, we extracted the temperature dependence of H_{c2} near T_c . Our results show good agreement with previous measurements by Kunchur *et al.* and Ossandon *et al.*,^{27,28} which are also plotted in Fig. 5. At temperatures much lower than T_c , however, no measurable MR in the YBCO film was observed. Therefore, at low temperatures where the junctions of Fig. 3 were measured, flux flow in the YBCO electrodes does not contribute to the MR. This conclusion holds, independent of the oxygen doping level of the YBCO.

*Electronic address: lior_shk@physics.technion.ac.il

¹P. G. deGennes, Rev. Mod. Phys. **36**, 225 (1964).

²G. Deutscher and P. G. deGennes, in *Superconductivity*, edited by R. D. Parks (Dekker, New York, 1966), pp. 1005–1034.

³M. Tinkham, *Introduction to Superconductivity*, 2nd edition (McGraw-Hill, New York, 1996).

⁴K. A. Delin and A. W. Kleinsasser, Supercond. Sci. Technol. **9**, 227 (1996).

⁵E. Polturak, G. Koren, D. Cohen, E. Aharoni, and G. Deutscher, Phys. Rev. Lett. **67**, 3038 (1991).

⁶A. Sharoni, I. Asulin, G. Koren, and O. Millo, Phys. Rev. Lett.

92, 017003 (2004).

⁷O. Neshor and G. Koren, Appl. Phys. Lett. **74**, 3392 (1999).

⁸O. Neshor and G. Koren, Phys. Rev. B **60**, 9287 (1999).

⁹G. Koren, L. Shkedy, and E. Polturak, Physica C **403**, 45 (2004).

¹⁰J. Bardeen and M. J. Stephen, Phys. Rev. **140**, A1197 (1965).

¹¹J. M. Ziman, *Electrons and Phonons* (Oxford University Press, London, 1960), Chap. XII.

¹²B. I. Shklovskii and L. Éfros, Sov. Phys. JETP **57**(2), 470 (1983).

¹³I. M. Lifshitz and V. Ya. Kirpichenkov, Sov. Phys. JETP **50**(3), 499 (1979).

¹⁴A. A. Abrikosov, Physica C **317–318**, 154 (1999).

- ¹⁵L. I. Glazman and K. A. Matveev, *Sov. Phys. JETP* **67**, 1276 (1988).
- ¹⁶L. Shkedy, P. Aronov, G. Koren, and E. Polturak, *Phys. Rev. B* **69**, 132507 (2004).
- ¹⁷K. Maki, in *Superconductivity*, edited by R. D. Parks (Dekker, New York, 1966), pp. 1035–1105.
- ¹⁸Y. Ando and K. Segawa, *Phys. Rev. Lett.* **88**, 167005 (2002).
- ¹⁹I. Lubimova and G. Koren, *Phys. Rev. B* **68**, 224519 (2003).
- ²⁰N. F. Mott, *Philos. Mag.* **26**, 1015 (1972); A. F. Ioffe and A. R. Regel, *Prog. Semicond.* **4**, 237 (1960); J. H. Mooij, *Phys. Status Solidi A* **17**, 521 (1973).
- ²¹T. Hashimoto, M. Sagoi, Y. Mizutani, J. Yoshida, and K. Mizushima, *Appl. Phys. Lett.* **60**, 1756 (1992).
- ²²C. Stozel, M. Siegel, G. Adrian, C. Krimmer, J. Stollner, W. Wilkens, G. Schulz, and H. Adrian, *Appl. Phys. Lett.* **63**, 2970 (1993).
- ²³A. Frydman and Z. Ovadyahu, *Europhys. Lett.* **33**, 217 (1996).
- ²⁴I. Bozovic, G. Logvenov, M. Verhoeven, P. Caputo, E. Goldobin, and M. R. Beasley, *Phys. Rev. Lett.* **93**, 157002 (2004).
- ²⁵N. Gedik, J. Orenstein, Ruixing Liang, D. A. Bonn, and W. N. Hardy, *Science* **300**, 1410 (2003).
- ²⁶A. R. Strnad, C. F. Hempstead, and Y. B. Kim, *Phys. Rev. Lett.* **13**, 794 (1964).
- ²⁷M. N. Kunchur, D. K. Christen, and J. M. Phillips, *Phys. Rev. Lett.* **70**, 998 (1993).
- ²⁸J. G. Ossandon, J. R. Thompson, D. K. Christen, B. C. Sales, H. R. Kerchner, J. O. Thomson, Y. R. Sun, K. W. Lay, and J. E. Tkaczyk, *Phys. Rev. B* **45**, 12 534 (1992).